GRAY STELLAR ATMOSPHERE MODEL FOR AN A0V STAR

December 1, 2018

ASTR 545

Oana Vesa

Contents

ABSTRACT

A one-dimensional, plane parallel, gray stellar atmosphere model in local thermal equilibrium of an A0V star was constructed. An A0V star is a main-sequence A-type star that has an effective temperature of 9520 K and a surface gravity of $\log g = 4.14$. It is composed of 70% Hydrogen, 29% Helium, and 1% Calcium. This stellar atmosphere is created with the assumption that convection does not play a huge factor in shaping the atmosphere. At an optical depth of about 10^0 to 10^1, a lot of interesting features are apparent. For instance, there is a noticeable increase in the opacities at around this range (seen in the form of a sharp rise), where they hit a maximum value before falling back down. Another interesting feature is that at around this range, the total mass density, nuclear pressure, total pressure, and gas pressure all sort of plateau. For an A0V star, the total pressure is mainly composed of the gas pressure, and radiation pressure starts playing a pertinent role in optically thick regions. Additionally, Hydrogen ionization and to some extent the beginning ionization of Helium plays a critical role in creating the interesting features discovered in the atmosphere at around the mentioned optical depth range.

METHODS

Many physical assumptions were employed in the creation of this A0V stellar atmosphere model. It is assumed that it is a one-dimensional, plane-parallel, gray atmosphere model in local thermal equilibrium. The stellar atmosphere for this A0V star was also built under the assumption that the star has an effective temperature of 9520 K, a surface gravity of $\log g = 4.14$, and has a solar composition. In other words, it is assumed that the star is composed of 70% Hydrogen, 29% Helium, and 1% Calcium.

A one-dimensional, plane-parallel atmosphere implies that the thickness of the atmosphere is much smaller than the star's radius. In other words, it is about 10^{-4} of the star's radius (see Module: Model Stellar Atmospheres, 2018). This also means that the only variable to take into consideration is optical depth.

Local thermal equilibrium is a good approximation for many stars, especially for optical depths greater than $\tau \geqslant 0.001$ (Module: Ionization Equilibrium, 2018; Owocki, 2010). A system in local thermal equilibrium means that the thermal properties that govern the body, such as gas and radiation do not vary much. In fact, they vary very little on short time scales when compared to the overall body that thermal equilibrium can be assumed. This also means that the radiation field is isotropic and described by the Planck function (see Module: Ionization

Equilibrium, 2016). Additionally, this allows ionization states to be described by the Saha equation and the excitation states to be described by the Boltzmann equation which are important for computing the opacities in the stellar atmosphere (see Module: Ionization Equilibrium, 2016).

The gray atmosphere model gives a simplified solution to the radiative transfer problem (Collins, 2003). With the Gray atmosphere model, mean opacities, $\overline{\chi}(\rho, T)$, are assumed. This allows the system to be simplified because opacities are heavily influenced by electron density, ionization conditions, temperature, and pressure. Thus, mean opacities can be used because in the gray atmosphere model, the opacity is assumed to be constant across all frequencies (Collins, 2003). In other words, the mean opacities are independent of wavelength or frequency.

Establishing an Optical Depth and Temperature Grid

This stellar atmosphere model was created by initially creating ten evenly spaced optical depth layers in log space. This was done by establishing an optical depth range of ten evenly spaced layers spanning from $10^{-3} \leqslant \tau \leqslant 10^{2}$. With this atmospheric grid established, the temperature per layer could be calculated. To do this, an interpolation of the temperature-tau relationship with the Hopf function was used. The temperature-tau relationship can be defined by

$$T^4(\tau) = \frac{3}{4} T_{\text{Teff}}^4 (\tau + q(\tau)), \tag{1}$$

where T_{Teff} is the effective temperature of the star, τ is the optical depth, and q is the Hopf function. This relationship is used under the assumption that the stellar atmosphere is a gray atmosphere using mean opacities; has isotropic radiation, which implies that all radiation intensity is the same in any direction; and that the atmosphere is under thermal and radiative equilibrium (see Module: Model Stellar Atmospheres, 2018). In order to obtain the temperatures for the atmospheric layers, the tau and Hopf functions were linearly interpolated from Table $3-2$ from Mihalas found in the module "Model Stellar Atmospheres" using SciPy in Python.

Establishing the Initial Pressure

Following the establishment of an optical depth and temperature grid, the pressures need to be determined. An iterative scheme was employed to solve for the pressure gradient in each layer. In order to initiate the iterative process, the boundary pressure, or the pressure for the

surface layer, ($\tau = 10^{-3}$), needed to be calculated. This boundary pressure was estimated by looking at the key figure 9.17 from Gray found in the module "Model Stellar Atmospheres" illustrating the gas pressure as a function of effective temperature of a solar-like star for several optical depths. This plot can be used because the gas pressure is approximately equal to the total pressure for very small τ values (see Module: Model Stellar Atmospheres, 2018).

By locating an approximate effective temperature of 9520 and $\log\tau$ value of -3, a boundary pressure of 1.8 dynes/cm^2 for the surface layer was obtained for a solar composition of $\log g = 4.0$. However, because an A0V star has a $\log g = 4.14$ value, a pressure-surface gravity scaling relationship had to be utilized. The pressure-surface gravity scaling relation can be defined as

$$\log P(\tau) = \log P^{'}(\tau) + \frac{2}{3}\left(\log g - \log g^{'}\right), \tag{2}$$

where $\log P^{'}(\tau)$ is the reference pressure obtained from the plot, $\log g$ is the star's surface gravity, and $\log g^{'}$ is the reference surface gravity from the plot ($\log g = 4.0$) (see Module: Model Stellar Atmospheres, 2018). By solving Equation 2, the initial pressure can be calculated.

Detailed Balancing

After calculating the boundary pressure and the temperature for the top layer, the total electron density, the total density, and the respective opacity of the layer has to be determined, as well. It is important to note that the density is dependent on the equilibrium balance of the charge conservation, or the electron density, while the opacity is dependent upon the total density and temperature of the layer. The electron density, defined by

$$n_e = (n - n_e)\sum_k \alpha_k \sum_{j=1}^{k+1}(j-1) f_{jk}, \tag{3}$$

can be solved by employing the root finding algorithm of Brent's method to solve for n_e. Python's SciPy's optimization module contains a small routine on Brent's root solving method.

However, in order to use Brent's method, it is imperative to compute the ionization fractions using the Saha equation. This can be completed using the recursive ionization fraction formula defined by

$$f_{jk} = f_{j-1,k} Y_{j-1,k}, \tag{4}$$

where the Saha equation is defined by

$$Y_{jk} = \frac{C_\phi}{n_e} \frac{U_{j+1,k}(T)}{U_{jk}(T)} T^{3/2} \exp\left(-\frac{\chi_{ijk}}{kT}\right). \tag{5}$$

In Equation 5, C_ϕ is a constant defined by $2\left(\frac{2\pi m_e k}{h^2}\right)^{3/2} = 4.83 \times 10^{15}$ cm^{-3}K$^{-3/2}$, U_{jk} is the partition function, and χ_{ijk} is the ionization potential.

After doing this detailed balancing and solving for the electron density, the total density, defined by

$$\rho_{total} = \sum_k n_k A_k m_{\text{amu}} + m_e n_e, \tag{6}$$

can be calculated by knowing n_k, the number density of species k (which refers to a specific metal); A_k, the atomic weight of species k; m_{amu}, the atomic mass weight (1.66054×10^{-24} g); m_e, the mass of an electron (9.10938×10^{-28} g); and n_e, the electron density. The number density of a particular species k is defined by

$$n_k = \alpha_k n_N, \tag{7}$$

where α_k is the abundance fraction and n_N is the number density of all atomic or nuclear particles. The abundance fraction is given by

$$\alpha_k = \frac{x_k/A_k}{\sum_k x_k/A_k}, \tag{8}$$

where x_k refers to the mass fraction of a particular species k; the number density of all atomic or nuclear particles can be found from solving for the nuclear pressure

$$P_N = n_N kT. \tag{9}$$

Because it is difficult to obtain the number density of all atomic or nuclear particles without knowing the nuclear pressure, the nuclear pressure can be solved using

$$P_N = \frac{k\rho T}{\mu_N m_{\text{amu}}}, \tag{10}$$

where μ_N the mean molecular weight for atomic and nuclear particles can be solved from

$$\mu_N = \left[\sum_k \left(\frac{x_k}{A_k}\right)\right]^{-1}. \tag{11}$$

Additionally, because the electron number density will be solved from Equation 3, the electron pressure can be solved from

$$P_e = n_e kT. \tag{12}$$

Another pressure that can also be determined is the radiation pressure given by

$$P_r = \frac{a}{3}T^4, \tag{13}$$

where a is the radiation density constant that is equal to 7.56×10^{-15} erg cm^{-3} K^{-4}. Moreover, the gas pressure can be obtained from adding the nuclear and electron pressures.

Furthermore, the Hydrogen excitation density fractions of $\frac{n_{111}}{n_1}$, $\frac{n_{211}}{n_1}$, and $\frac{n_{311}}{n_1}$ can be derived by using Equation 5,

$$\frac{n_{ijk}}{n_{jk}} = \frac{g_{ijk}}{U_{jk}(T)} \exp\left(-\frac{\chi_{ijk}}{kT}\right) \tag{14}$$

and

$$\frac{n_{ijk}}{n_k} = \frac{n_{ijk}}{n_{jk}} f_{jk}, \tag{15}$$

where for instance,

$$\frac{n_{211}}{n_1} = \frac{n_{211}}{n_{11}} \left(\frac{1}{1+Y_{11}}\right). \tag{16}$$

In Equation 14, g_{ijk} is the statistical weight given by

$$g_{ijk} = 2n^2 \tag{17}$$

(where n corresponds to i); and χ_{ijk} is the excitation energy that is given by

$$\chi_{ijk} = R_H \left(1 - \frac{1}{n^2}\right) \tag{18}$$

and R_H is the Rydberg constant of 13.598 eV.

Determining the Mean Opacity

The total density found from Equation 6 can be used to solve for the opacity of the atmospheric layer, $\chi(\rho_{\text{total}}, T)$. The Rosseland mean opacities are most commonly utilized for simple stellar atmospheric models even though it does have its faults and is not robust for

more complex models (see Module: Model Stellar Atmospheres, 2018). However, given a simplified Gray atmosphere, the Rosseland mean opacities derived from The Opacity Project (OPAL) tables are a good fit (Iglesias & Laboratory, 2001). These opacity tables are in terms of $\log R$ (ranging from -8.0 to 1.0) versus $\log T$ (ranging from 3.75 to 8.70), where the R values can be derived from

$$R = \frac{\rho}{T_6^3}, \tag{19}$$

where $T_6 = \frac{T}{10^6}$ K and ρ is the density in g/cm^3. By knowing the $\log R$ and $\log T$ values, the mean opacities can be determined. OPAL Table #72 was used for this stellar atmosphere.

However, it is imperative to interpolate the table to match the temperature values determined from Equation 1. Using a combination of the linear interpolation packages in NumPy and SciPy, the OPAL Table #72 was interpolated. Given that there are 70 values of $\log T$'s, the $\log R$ values were linearly interpolated (using NumPy's linear interpolation routine) with their corresponding opacities to construct a new array that matched the number of values of the temperature array. As a result, a new opacity table was constructed that was size 70×70.

To obtain the opacity value for each atmospheric layer, a function was created that first determined the closest $\log R$ value from Table #72 to the $\log R$ value calculated from Equation 19. This function printed out the column number corresponding the the closest $\log R$ value. Using this column number along with the temperature of the layer, another linear interpolation was performed using SciPy's interpolation routine for the temperature to obtain an opacity value that matched the layer's temperature.

The Pressure Gradient

After solving the detailed balancing of the current layer to obtain the total pressure, the total density, and the total opacity, the subsequent layer can be solved. For each of the layers following the top layer, an interactive scheme was employed to solve for the pressure gradient. To begin the process, an initial guess of

$$P_i^{'} = P_{i-1} + g\left(\frac{\tau_i - \tau_{i-1}}{\chi(\rho_{i-1}, T_{i-1})}\right) \tag{20}$$

for the pressure gradient must be made using the previous layer's information. Using this pressure estimate, all of the necessary detailed balancing is calculated for the current layer. However, this estimate is likely incorrect; thus, to obtain a value closer to the correct pressure

value, a new guess for the pressure,

$$P_i^{''} = P_{i-1} + 2g\left(\frac{\tau_i - \tau_{i-1}}{\chi\left(\rho_{i-1}, T_{i-1}\right) + \chi^{'}\left(\rho_i^{'}, T_i\right)}\right), \tag{21}$$

must be obtained where the mean opacities are averaged.

Essentially, to obtain the correct pressure, the pressure gradient must satisfy the hydrostatic equilibrium conditions of

$$P_{i+1} = P_i + 2g\left(\frac{\Delta\tau_i}{\overline{\chi}_i + \overline{\chi}_{i+1}^{'}}\right) \tag{22}$$

and

$$P_i = P_{i+1} - 2g\left(\frac{\Delta\tau_i}{\overline{\chi}_i^{'} + \overline{\chi}_{i+1}^{'}}\right). \tag{23}$$

Once hydrostatic equilibrium is achieved, the last pressure calculated is the total pressure for that layer and the next layer can be solved.

If hydrostatic equilibrium is not achieved, continue creating pressure guesses using Equation 21 by averaging the mean opacities and solve for the pressure gradient again. To reach hydrostatic equilibrium for each layer, a convergence routine is needed. The convergence routine will go through all of the detailed balancing of the layer to refine the pressure value a certain number of times until the pressure gradient guesses from Equation 21 converge to an established threshold value illustrated by

$$\frac{|P_i^{''} - P_i^{'}|}{P_i^{'}} \leqslant \epsilon, \tag{24}$$

where ϵ is the threshold factor that is set at 10^{-5}. When this threshold value is reached, then the routine acknowledges that the pressure has converged to a value that satisfies the hydrostatic equilibrium shown in Equations 22 and 23. As mentioned above, once this value is reached, this is the total pressure for the current layer, and the next layer can be solved. If not, the entire process is repeated until convergence has been made.

Algorithm

The following details an algorithm for solving for the solution that sums up all of the above subsections:

- Define the star for which to create a gray stellar atmosphere making sure to have an effective temperature, surface gravity, mass fractions, the corresponding Rosseland mean opacity table for those mass fractions, and boundary conditions.
- Set up the temperature and optical depth grids by interpolating Equation 1.
- Obtain the total pressure for the top layer. Appropriately scale it using Equation 2 to match the chosen star's surface gravity.
- After calculating the total pressure for the top layer, solve the detailed balancing of that layer to obtain the total density, electron density, pressures, ionization fractions, and the mean opacity using an interpolated OPAL opacity table.
- Solve for the detailed balancing of subsequent layer by first obtaining an initial pressure guess using Equation 20. Use information from the previous layer to calculate this and then find the total density and mean opacity for that new pressure guess.
- Refine the pressure gradient using Equation 21 using averaged opacities to ensure that the hydrostatic equilibrium as seen in Equations 22 and 23 is satisfied.
- Create a convergence routine using the pressure guesses for the condition seen in Equation 24 using a threshold value of 10^{-5}.
  - If the condition is met, then set $P_i = P_i^{''}$ and solve for the next layer.
  - If the condition is not met, then set $P_i^{'} = P_i^{''}$ and solve for the pressure gradient again until the condition is satisfied.

RESULTS

Tables

The following tables list the values of optical depth, physical depth, temperature, opacity, total mass density, gas pressure, electron pressure, electron density, neutral Hydrogen ionization fractions, and the Schwarzschild Criterion derived from the code. These values are mostly discussed in the following subsection entitled "Figures". The results of Table 3 are discussed in the last subsection entitled "Schwarzschild Criterion".

Optical Depth	**Physical Depth**	**Temperature (K)**	**Opacity (cm^2/g)**	**Total Mass Density (g/cm^{-3})**
0.00100	0	7729.44	0.66938	8.047×10^{-11}
0.00359	4.815×10^7	7747.47	0.67021	1.645×10^{-10}
0.01291	1.326×10^8	7807.10	0.83351	5.228×10^{-10}
0.04641	2.095×10^8	7971.50	1.29661	1.299×10^{-9}
0.16681	2.810×10^8	8402.59	3.20189	2.097×10^{-9}
0.59948	3.454×10^8	9432.99	13.72002	1.868×10^{-9}
2.15443	4.060×10^8	11523.85	35.85726	1.792×20^{-9}
7.74263	4.930×10^8	15106.20	12.32841	5.056×10^{-9}
27.82559	8.151×10^8	20476.25	12.86450	2.564×10^{-8}
100.0000	1.033×10^9	28065.37	25.60347	4.403×10^{-8}

Table 1: The table above displays the main physical quantities (optical depth, physical depth, temperature, opacity, and total mass density) for the gray stellar atmosphere of the A0V star.

Gas Pressure ($dynes/cm^{-3}$)	**Electron Pressure ($dynes/cm^{-3}$)**	**Electron Density (cm^3)**	**Neutral Hydrogen Ionization Fraction**
50.607	10.932	1.024×10^{13}	0.82112
98.211	16.887	1.578×10^{13}	0.87051
295.033	34.656	3.215×10^{13}	0.92053
731.489	70.9369	6.445×10^{13}	0.93685
1284.570	160.535	1.383×10^{14}	0.91423
1555.804	431.264	3.311×10^{14}	0.73381
2430.805	1113.054	6.995×10^{14}	0.17236
9410.139	4537.507	2.175×10^{15}	0.01649
65943.091	32450.995	1.147×10^{16}	0.00419
156473.519	77640.289	2.003×10^{16}	0.00056

Table 2: The table above displays the results of the detailed balancing (electron density and neutral Hydrogen ionization fraction) and various pressures (gas and electron pressure) of the gray stellar atmosphere of a A0V star.

Layer	$r_d \nabla_r$	∇_{ad}	**Stable Against Convection?**
1	0.003424	0.296546	Yes
2	0.006502	0.290932	Yes
3	0.020109	0.285339	Yes
4	0.059573	0.283540	Yes
5	0.174755	0.286036	Yes
6	0.434830	0.306626	No
7	0.589434	0.372266	No
8	0.253681	0.390631	Yes
9	0.538971	0.399497	No
10	0.715408	N/A	N/A

Table 3: The table above displays the results of the Schwarzschild Criterion indicating if the layer is stable against convection or not. If $\Delta_{ad} < r_d \nabla_r$, then layer is stable against convection. If $\Delta_{ad} > r_d \nabla_r$, then the layer is unstable to convection.

Figures

The following figures highlight the results obtained from the code, as seen in Tables 1, 2, and 3.

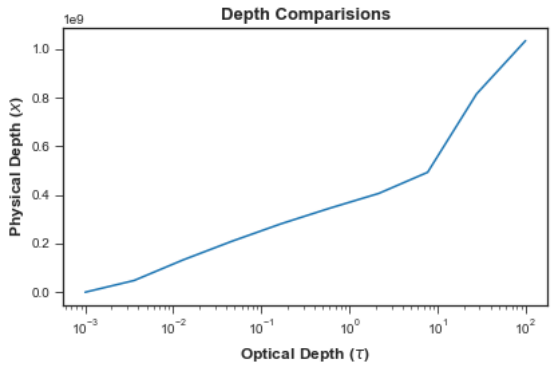

(a) Physical Depth, x, versus optical depth, τ

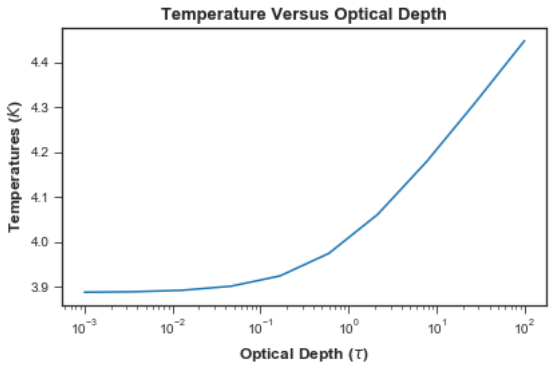

(b) Temperature, T, versus optical depth, τ

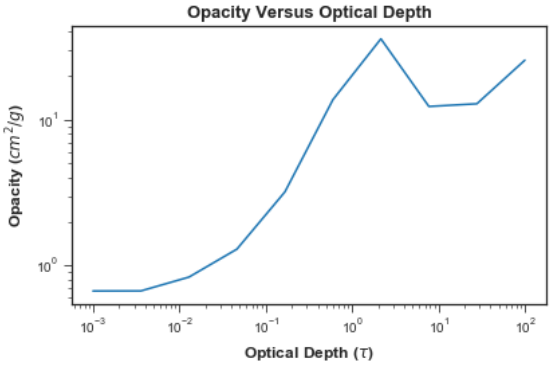

(c) Opacity, $\chi^{'}$, versus optical depth, τ

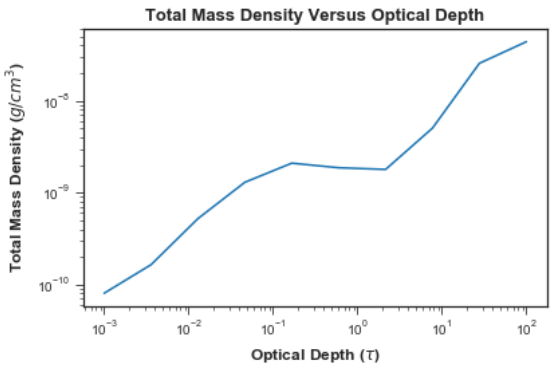

(d) Total mass density, ρ, versus optical depth, τ

Figure 1: The plots above illustrate how the main physical quantities (from left to right in each row) of physical depth, temperature, opacity, and total mass density, seen in the gray stellar atmosphere of an A0V star vary with optical depth.

Figure 1a illustrates how physical depth varies with optical depth. The overall trend exhibited is that as physical depth increases, optical depth increases. Essentially, the further within a star's atmosphere the photons travel, the more optically thick the layers become. An interesting feature to point out is that at around an optical depth of 10, the physical depth increases drastically while in the optically thin regions, there is only a gradual increase of physical depth.

Figure 1b depicts the variation in temperature versus the optical depth. As should happen, as the optical depth increases, the temperature increases. Optically thick regions are closer to

the core of the star, which is known to be hotter in general. Therefore, it makes sense that temperature would increase the closer to the core the layer is. An interesting aspect of this plot to point out is that at an optical depth of around 10^0, the temperature starts to increase more rapidly than before.

In Figure 1c, it can be elucidated that overall in optically thick regions, the opacity will increase. An important part of this plot to notice is the bump at around an optical depth of 10^0. When compared to the reference plots handed out as part of the assignment, this figure is incorrect because there should be a smooth bump at an optical range of $10^0 - 10$, and the opacity should not start rising up again at the end. This is not physically feasible. This is most likely the result of an interpolation error. However, it is interesting to note that the opacity reaches a maximum value at around the optical depth when Hydrogen starts becoming ionized, as seen in Figure 3.

Figure 1d shows that as optical depth increases, total mass density increases, as well. Thus, the more optically thick regions have a higher total mass density. Furthermore, it is interesting to note that the total mass density is pretty constant from optical depths of around 10^{-1} to 10. This mirrors the behavior of the nuclear (and to some extent the total and gas pressure) in Figure 2. This pressure-density relationship is also exhibited in Equation 10. Essentially, as pressure increases, density should follow suit, as well.

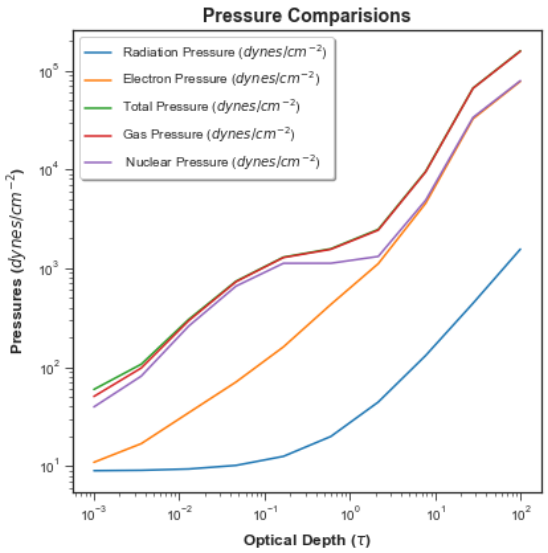

(a) Total pressure, gas pressure, nuclear pressure, electron pressure, and radiation pressure versus optical depth, τ

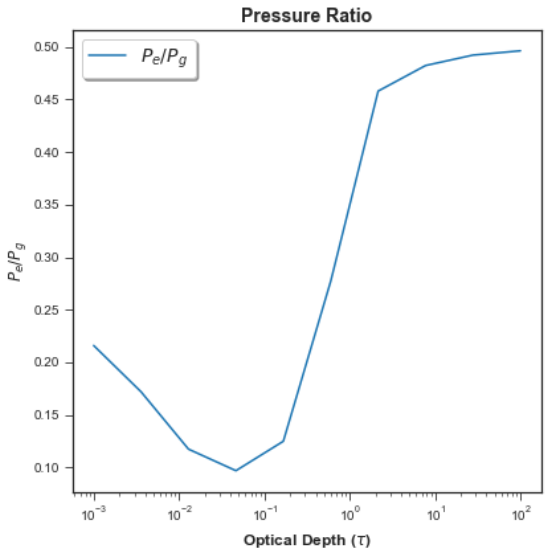

(b) The ratio of electron pressure (dynes/cm^{-3}) and gas pressure (dynes/cm^{-3}) versus optical depth, τ

Figure 2: The plots above show the variation of various pressures (radiation,electron,total,gas,and nuclear) with optical depth.

In Figure 2a, the overall trend is that the pressures will increase as optical depth increases. It is interesting to note that gas pressure (red line) and total pressure (green line) are essentially the same after an optical depth of around 10^{-2}, which implies that gas pressure makes up most of the total pressure in a gray stellar atmosphere of an A0V star. Another interesting thing to point out is that electron pressure (orange line) and nuclear pressure (purple line) also become the same at around an optical depth of 10. Furthermore, as mentioned when discussing Figure 1d, nuclear pressure and to some extent the total and gas pressure mirror the curve of the total mass density. Moreover, another important feature to elucidate is that there is very little radiation pressure (blue line) in the atmosphere in the optically thin regions. However, once the optical depth increases and it becomes an optically thick regime, the radiation pressure increases rapidly indicating that radiation pressure is important in optically thick regions and plays a bigger role in later layers of the atmosphere.

Figure 2b shows the ratio of electron and gas pressure as optical depth increases. It is important to note that this ratio approaches a value of 0.5 at an optical depth of 10^0, which is when the temperature really starts to increase (as seen in Figure 1b) at a temperature of around 10,000 K. This is also the location where, as seen in Figure 3, Hydrogen starts to becoming fully ionized and Helium is starting to become ionized and contributing to the atmosphere.

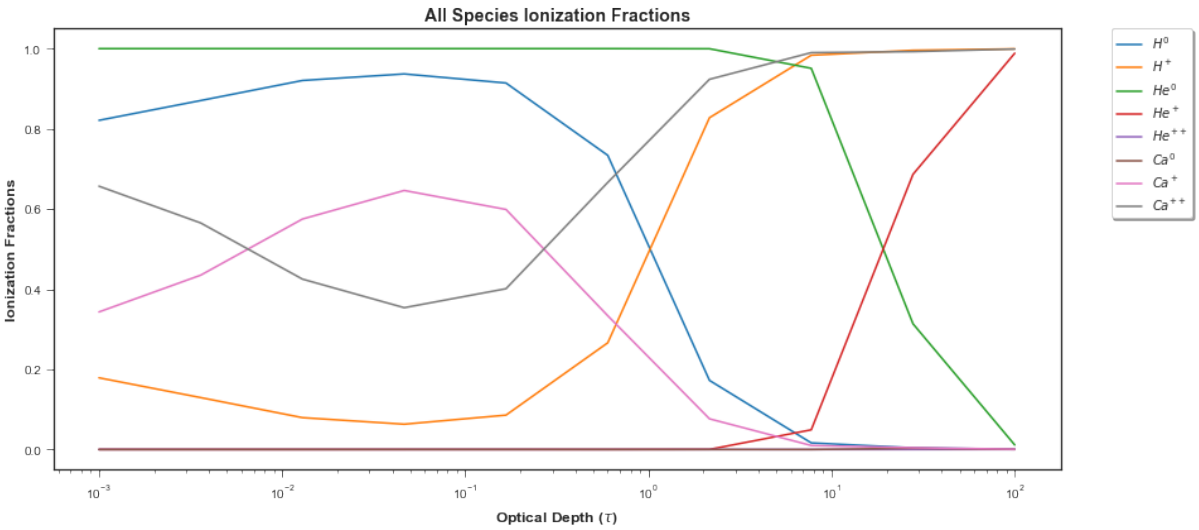

Figure 3: The plot above shows the different ionization fractions, $f_{jk} = n_{jk}/n_k$, of Hydrogen, Helium, and Calcium versus optical depth, τ.

Figure 3 shows that most ionization occurs after an optical depth of 10^0. It is interesting to note that there is little to no neutral Calcium (brown line) and doubly ionized Helium (purple

line) in the gray stellar atmosphere of an A0V star. Another facet of this plot is that Calcium starts becoming doubly ionized early on in optically thin regions, so there is a lot of ionized Calcium contributing to the earlier part of the gray stellar atmosphere. Moreover, Hydrogen starts becoming ionized at an optical depth of 10^0 (blue line) and Helium at an optical depth of around 10 (red line). The optical depth of 10^0 is really important for this stellar atmosphere because as seen in the previous plots, the most interesting aspects of the atmosphere happen around this optical depth. This implies that the ionized Hydrogen contributes a lot to the overall features of the stellar atmosphere.

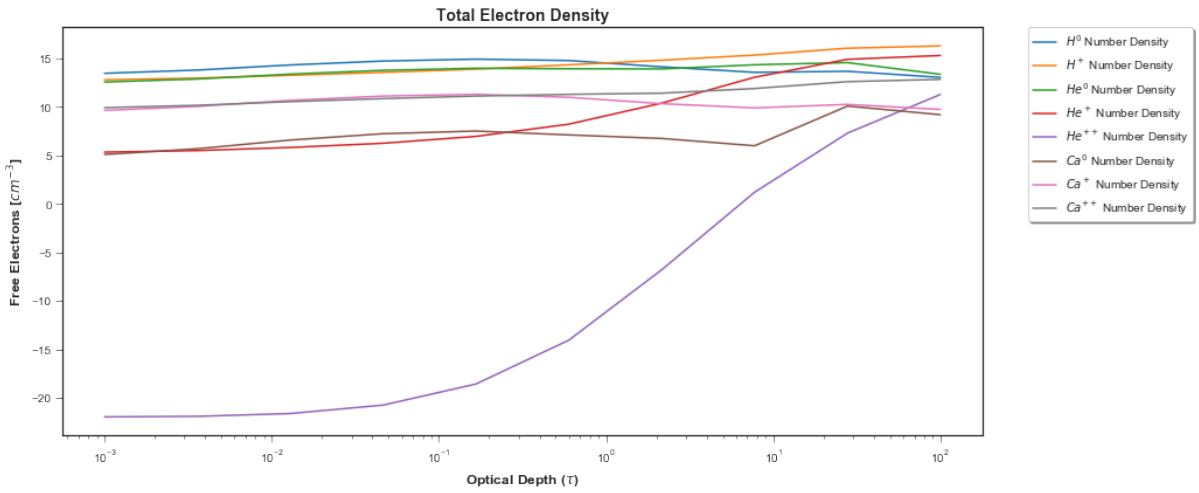

Figure 4: The plot above shows the free electrons, n_e derived from each n_{jk} of Hydrogen, Helium, and Calcium versus optical depth, τ.

Figure 4 shows how the total electron density of each metal in the stellar atmosphere varies with optical depth. Overall, there is a lot of free electrons contributed from the Hydrogen and Calcium ions. Additionally, for the most part, the number of free electrons in the neutral and excited state of Hydrogen (blue and orange lines, respectively) do not vary drastically as optical depth increases. At around the optical depth of 10^0, the total number of free electrons for the singly ionized Hydrogen increases because this is when Hydrogen starts becoming ionized as seen in Figure 3. Another interesting feature of this plot to point out is the free electron contribution of doubly ionized Helium (purple line). In comparison to the previous figure, Figure 3, which had no ionization fraction contributions from this ion, doubly-ionized Helium contributes a lot of free electrons starting at an optical depth of 10^0.

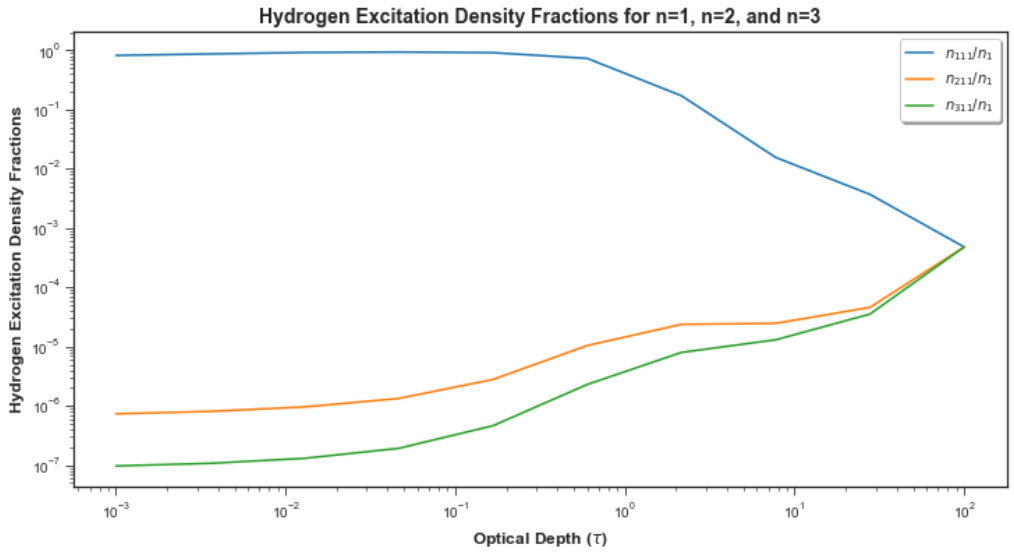

Figure 5: The plot above shows how the hydrogen excitation density fractions for $n_{111}/n_1, n_{211}/n_1$, and n_{311}/n_1 varies with increasing optical depth, τ.

Figure 5 illustrates how the various Hydrogen excitation density fractions vary with increasing optical depth. For the most part, there is a lot more excited Hydrogen in the first state (blue line) in comparison to the second and third state (orange and green line, respectively). However, at an optical depth of around 10^0, the second and third excited states start to increase and play more of a role in optically thick regions than the first excited state which decreases. Something interesting to point out is that at an optical depth of 10^2, all three excited states of Hydrogen end up meeting. It is difficult to tell the exact reason for this, and it could very well differ if the optical depth were to extend past 10^2. However, this plot shows that Hydrogen plays a big role within the stellar atmosphere of an A0V star.

Schwarzschild Criterion

The Schwarzschild Criterion describes if a particular layer in the stellar atmosphere is stable against convection. The Schwarzschild Criterion states that

- If $\nabla_{ad} < r_d \nabla_r$, then layer is stable against convection
- if $\nabla_{ad} > r_d \nabla_r$, then layer is unstable to convection (see Module: Stellar Hydrodynamics, 2016b),

where ∇_r is the radiative gradient and ∇_{ad} is the adiabatic gradient. The adiabatic gradient refers to an energy transport where there are no radiation losses while the radiative gradient

refers to an energy transport governed by radiation (see Module: Stellar Hydrodynamics, 2016b). The r_d term is a correction factor that is applied to the radiative gradient as a unity correction factor for optical depths greater than 0.5 (see Module: Stellar Hydrodynamics, 2016a).

The adiabatic gradient is given by the equation

$$\nabla_{ad} = \frac{1 + \frac{1}{\beta^2}(1-\beta)(4+\beta)}{\frac{5}{2} + \frac{4}{\beta^2}(1-\beta)(4+\beta)}, \tag{25}$$

where $\beta = \frac{P_{\text{gas}}}{P}$. The radiative gradient is given by

$$\nabla_r = \frac{3}{16}\frac{\kappa P}{g}\left(\frac{T_{\text{teff}}}{T}\right)^4, \tag{26}$$

where κ is the mass absorption coefficient (the Rosseland mean opacity), P is the pressure per layer, g is surface gravity, T is the temperature per layer, and T_{Teff} is the effective temperature of the star. The correction factor used to model stellar atmosphere is given by

$$r_d = 1 + \frac{dq(\tau)}{d\tau}, \tag{27}$$

where this is the departure from the diffusion approximation, and the $\frac{dq(\tau)}{d\tau}$ portion of this equation comes from Equation 1 (see Module: Stellar Hydrodynamics, 2016a).

As seen from the results of Table 3, layers 1 to 5 and layer 8 are stable against convection (where layer 1 is defined as the top layer), but layers 6,7,and 9 are unstable to convection. The last layer could not be determined because there is no information about future layers in order to be able to calculate the correction factor in Equation 27, which requires information about the next optical depth.

It is interesting to note that layer 8 is stable against convection while the previous two layers and the next layer are not; however, given that the radiative gradient depends on the mass absorption coefficient, or the opacity, it is reasonable because my opacities seen in Figure 1c are a tad off in the optically thick regions. This was likely due to some interpolation error. Therefore, I believe that if the opacity actually exhibited the correct bump at the optically thick portion of the atmosphere, then layer 8 would be unstable to convection, as well.

CONCLUSION

A gray stellar atmosphere with ten layers of an A0V star was created. The assumptions used to create this atmosphere was intended to simplify the stellar model. The stellar atmosphere of an A0V star has some interesting features appearing at around an optical depth range of 10^0 to 10. In this optically thick region, the opacities reach a maximum value (seen in the form of a sharp bump), total mass density mirrors nuclear pressure (and to some extent the total and gas pressure), and the ratio of electron and gas pressure reaches a value of 0.5. All of these features are mostly likely due to the fact that Hydrogen becomes fully ionized in this optically thick region and that Helium begins to become ionized. These ions contribute a lot to the formation of the stellar atmosphere in the optically thick regions. Also, the Schwarzschild Criterion was applied, and it was found that the optically thick regions are unstable to convection.

Further improvements to take into account to increase the realism of the model would be to modify this code to take into account more metals, to look at other types of stars that are not of a solar composition, and to look at giants and supergiants. The code would also be more robust if convection was allowed to play a role in the atmosphere.

Bibliography

Collins, G. W. 2003, in The Fundamentals of Stellar Astrophysics, 253 – 290

Iglesias, C., & Laboratory, L. L. N. 2001, OPAL Opacity Tables

Module: Ionization Equilibrium. 2016, Radiative and Collisional Processes

—. 2018, Radiative Process (Absorption/Emission)

Module: Model Stellar Atmospheres. 2018, The 1-D Plane-Parallel Stellar Atmosphere

Module: Stellar Hydrodynamics. 2016a, Basic Gas Physics

—. 2016b, Thermodynamics and Atmosphere Gradients

Owocki, S. 2010, PHYS-633: Introduction to Stellar Astrophysics